Journal of Electrochemical Science and Technology
Vol. 2, No. 2, 2011, 76-84
http://dx.doi.org/10.5229/JECST.2011.2.2.076

Journal of Electrochemical Science and Technology

Effect of Phosphoric Acid on the Electronic and Diffusion Properties of the Anodic Passive Layer Formed on Pb-1.7%Sb Grid of Lead-acid Batteries

H.A. Abd El-Rahman†, S.A. Salih, and A. M. Abd El-Wahab
Chemistry Department, Faculty of Science, Cairo University, Postal code 12613 Giza, EGYPT

ABSTRACT:

Potentiostatic oxidation of Pb-1.7%Sb alloy used in the manufacture of grids of lead-acid batteries over the potential range from −1.0 V to 2.3 V in 5 M H_2SO_4 in the absence and the presence of 0.4 M H_3PO_4 and the self-discharge characteristics of the oxide layer formed is studied by electrochemical impedance spectroscopy (EIS). Depending on the potential value, sharp variations in resistance and capacitance of the alloy are recorded during the oxidation and they can be used for identification of the various substances involved in passive layer. Addition of H_3PO_4 is found to deteriorate the insulating properties of the passive layer by the retardation of the formation of $PbSO_4$. H_3PO_4 completely inhibits the current and impedance fluctuations recorded in H_3PO_4-free solutions in the potential range 0.5 V-1.7 V. These fluctuations are attributed to the occurrence of competitive redox processes that involve the formation of $PbSO_4$, $PbOSO_4$, PbO and PbO_2 and the repeated formation and breakdown of the passive layer. Self-discharge experiments indicate that the amount of PbO_2 formed in the presence of H_3PO_4 is lesser than in the H_3PO_4-free solutions. The start of transformation of $PbSO_4$ into PbO_2 is greatly shortened. H_3PO_4 facilitates the diffusion process of soluble species through the passive layer ($PbSO_4$ and basic $PbSO_4$) but impedes the diffusion process through PbO_2.

Keywords: Pb-Sb alloy; Lead-acid cell; Phosphoric acid; potentiostatic oxidation; Self-discharge.

Received February 24, 2011 : Accepted June 20, 2011

1. Introduction

Phosphoric acid is an interesting additive to the sulphuric acid electrolyte used in lead-acid batteries to improve the performance.[1-22] Other additives, such as, boric acid,[22] mixture of H_3PO_4 and H_3BO_3,[23-25] metal cations[26-37] and organic compounds[38,39] were also proposed. H_3PO_4 is reported to be helpful in reduction of the sulfation after deep discharge,[1,7-10] increasing the life cycle,[1,7,8,15] slowing down the discharge.[14] It decreases the capacity[11] and increases the overpotentials of both hydrogen and oxygen evolution reactions.[14,16,17] Some electrochemical studies have indicated improvement of the formation of PbO_2 with the addition of H_3PO_4[13,14] but the results of other studies supported the opposite effect.[5,7,11,14,22]

One of the main reasons of the lead-acid battery failure is the severe corrosion of the anode grid during service due to the self-discharge. The effect of H_3PO_4 addition on the performance of the battery grids under oxidation and during the self-discharge seems to be an important part in the evaluation of H_3PO_4 as an economic electrolyte additive. In the present study the effect of H_3PO_4 on the nature of the products formed potentiostatically on Pb-1.7%Sb alloy and the self-discharge of the anode is studied by EIS.

†Corresponding author. Tel.: +202-35676565
E-mail address: abdelrahman_hamid@hotmail.com

2. Experimental

The electrodes were manufactured from a commercial low-antimony caste alloy rods (nominal composition Pb-1.7%Sb). The alloy is used in the wet lead-acid car batteries as grids to hold the active paste materials, and supplied by Chloride, Egypt for Batteries. It has the following composition: 97.68% Pb, 1.697% Sb, 0.149% As, 0.014% Se, 0.028% Cu, 0.013% Bi, 0.002% Ag. Cross sectional area of 0.11 cm^2 was only left to contact the test solution. The electrodes were mechanically polished with successive grades of emery papers up to 1200 grit, washed with acetone first and then doubly distilled water and finally wrapped with a fine tissue so that the surface appeared bright and free from defect. Chemically ultra-pure 98% sulfuric acid and 85% phosphoric acid stock solutions were used for preparation of solutions by the appropriate dilution with doubly distilled water.

Measurements were conducted in unstirred naturally aerated 5.0 M H_2SO_4 acid solutions in the absence and presence of 0.4 M phosphoric acid at constant temperature of 25 ± 0.2 °C. The different electrochemical measurements were carried using IM6 Zahner electric, Meβtechink, Germany. The electrode potential was measured versus a Hg/Hg_2SO_4/1 M H_2SO_4 reference electrode (0.680 V vs. SHE). A Pt sheet (2.0 × 2.0 cm^2) was used as a counter electrode. Impedance measurements at a fixed frequency of 1.0 kHz were recorded using an ac potential of 3 mV peak to peak. The measurements revealed the impedance, Z (Ω), and the phase shift angle, θ. The corresponding capacitance, C (F) and resistance, R (Ω) values were extracted from Z and q values. Impedance data were averaged automatically for 10 times before recording to improve the sensitivity. EIS data were recorded at the specified potentials in the frequency range from 0.1 Hz to 50 kHz. They were fitted with the appropriate equivalent circuits using the "SIM" program included with the IM6 package. SIM allows the construction of the equivalent circuit, performs the fitting of the experimental data and outputs the values of the elements involved in the equivalent circuit. The suitability of the elements in the equivalent circuit was judged by the error% of the fitting, comparison of the calculated and experimental impedance plots and the expected element value.

The impedance of the 3-electrode cell used in this study is reduced to that of the working electrode (the alloy under study) beside the solution resistance between the working and the counter electrodes. This is because of the impedance of the large area Pt electrode can be neglected compare to that of the much smaller alloy. With the formation and thickening of a dielectric or resistive substance on the alloy surface the electrical capacitance at a fixed frequency of the alloy should decrease according to the model of the parallel plate condenser. Meanwhile the electrical resistance should increase according to the resistor model. The transformation of an insulating layer into a conducting one is expected accordingly to show an increase in capacitance and a decrease in resistance.

3. Results and Discussion

3.1. Potentiostatic oxidation in the absence and presence of H_3PO_4

Pb-1.7%Sb electrode was reduced at −1.2 V in 5 M H_2SO_4 for 5 minutes to remove any naturally formed passive films. Then the electrode potential was steeped to specified oxidation potentials, E_{ox} (in the range from −1.0 V to 2.2 V) and the instantaneous current, I, capacitance, C, and resistance, R, were recorded. The variations in I, C and R with time are shown in Fig. 1. Due to the

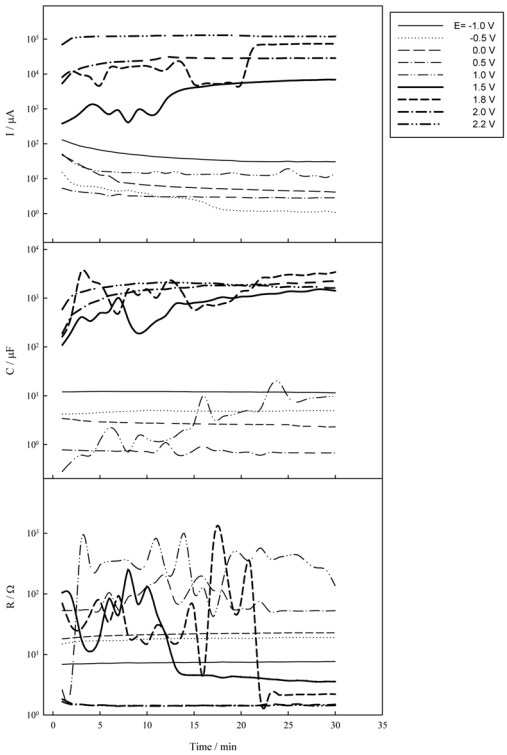

Fig. 1. Variation of the instantaneous current, I, capacitance, C, and resistance, R, of Pb-1.7%Sb alloy with time in 5 M H_2SO_4 at different electrode potentials.

large effect of E_{ox} on I, C and R the logarithms of their values are used in the figure. At −1.0 V I and C initially decrease with time while R increases and then quasi-steady values were reached after ~15 minutes. C shifts towards lower values while R shifts towards higher values as E_{ox} increases up to 0.5 V. Meanwhile I shifts from negative values at −1.0 V to positive increasing values as E_{ox} increases. These changes indicate the formation and the growth of an insulating layer of $PbSO_4$.[39,40]

In the E_{ox} range from 0.5 V to 1.8 V strong fluctuations in I, C and R can be seen, although thickening of the porous passive layer can easily be deduced (lower I and C and higher R) . These fluctuations ceased after ~ 30 minutes and at E_{ox} > 1.8 V. They are attributed to the competitive redox processes involved in the formation and the transformations of the predominately insulating Pb(II) compounds into the conducting PbO_2. Thermodynamically, the transformations of $PbSO_4$ and PbO into PbO_2 start at 0.96 V and 0.38 V, respectively, in 5 M H_2SO_4 solution.[39,40] Substantially higher C and I and lower R values can be seen at E_{ox} > 1.5 V and they indicate the complete coverage of the alloy surface with a conducting porous PbO_2 layer.

The effect of addition of H_3PO_4 to 5 M H_2SO_4 on the instantaneous I, C and R at some selected E_{ox} values is shown in Fig. 2. At −1.0 V, C and I decreases with time while R increases as observed for the H_3PO_4-free solution. The quasi-steady I, C and R values after 30 minutes in the absence and presence of H_3PO_4 are, respectively, 30 μA & 110 μA, 11.5 μF & 26.5 μF and 7.7 Ω & 6.7 Ω. These values indicate a thinner $PbSO_4$ layer in the presence of H_3PO_4. The most pronounced effect of addition of H_3PO_4 is the disappearance of the fluctuations recorded in the H_3PO_4-free solution. At E_{ox} = 0.5 V I increases at the beginning up to 2 minutes, then it deceases slowly. Meanwhile C decreases with time and R increases. The peak-shaped current transient is characteristic for the nucleation and the 3-dimentional growth of passive layers.[41] This behavior is absent for the H_3PO_4-free solution. The behavior may be attributed to the nucleation and 3-dimensional growth of some $PbHPO_4$ grains together with the deposition of the insulating $PbSO_4$, possible at 0.5 V and higher.[20,21] The presence of $PbHPO_4$ seems to be the reason of disappearance of the fluctuations.

Fig. 3 summarizes the dependence of the steady I, C and R on E_{ox} in the absence and the presence of H_3PO_4. The general behaviour is the same in the two solutions. The minimum C value occurs at 0.5 V in both solutions, but

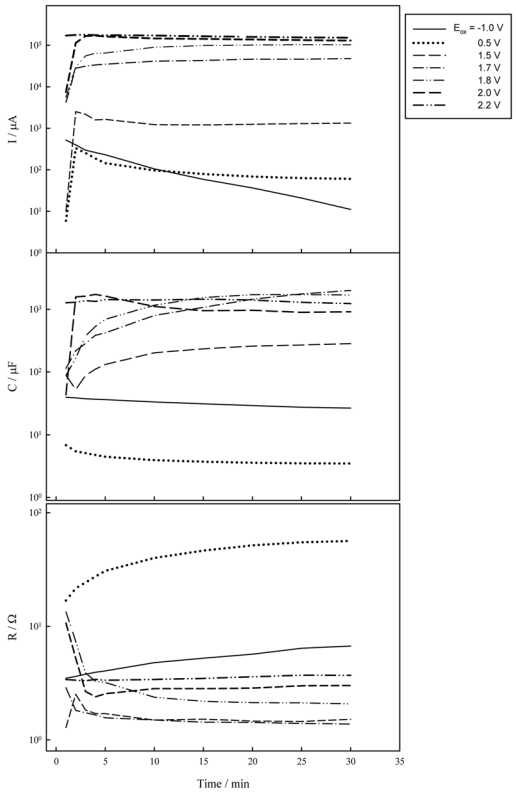

Fig. 2. Variation of the instantaneous current, I, capacitance, C, and resistance, R, of Pb-1.7%Sb alloy with time in 5 M H_2SO_4 + 0.4 M H_3PO_4 at different electrode potentials.

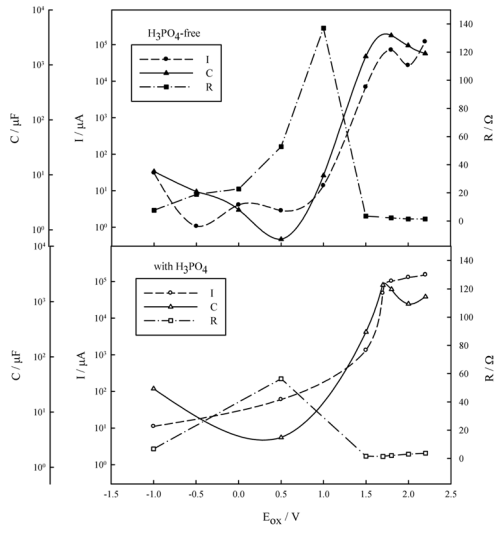

Fig. 3. Quasi-steady I, C, and R of Pb-1.7% alloy versus the oxidation potential, E_{ox} in 5 M H_2SO_4 in the absence (Closed symbols, Upper) and the presence of 0.4 M H_3PO_4 (Open symbols, Lower). Data were extracted from Figs. 1 & 2 after 30 minutes of oxidation.

higher in the presence of H_3PO_4. This is consistent with a thinner passive layer in the presence of H_3PO_4. It is interesting to see that the maximum R occurs at 1.0 V with a corresponding C value that is comparable to C value at −1.0 V. This indicates the absence of any significant amounts of PbO_2. At $E_{ox} \geq 1.5$ V, the formation of the conducting PbO_2 is accompanied by a very sharp increase in both I and C and a sharp decrease in R. R values in both solutions (1.4-3.5 Ω) are practically the solution resistances and they are even lower than the resistances at the corrosion potentials (6.7-7.7 Ω). This is because a thin insulating $PbSO_4$ layer exists at the corrosion potential while a conducting PbO_2 is formed at $E_{ox} \geq 1.5$ V.

Impedance spectra were recorded after 30 minutes at some selected E_{ox} values in 5 M H_2SO_4 in the absence and the presence of 0.4 M H_3PO_4 and examples are shown in Fig. 4. These plots reflect the electrical properties and the redox processes involved at the specified potentials. At E_{ox} 0.5 V, log Z-log f plots shift towards higher values as E_{ox} increases, indicating the improvement of the insulating properties of the $PbSO_4$ passive layer. The

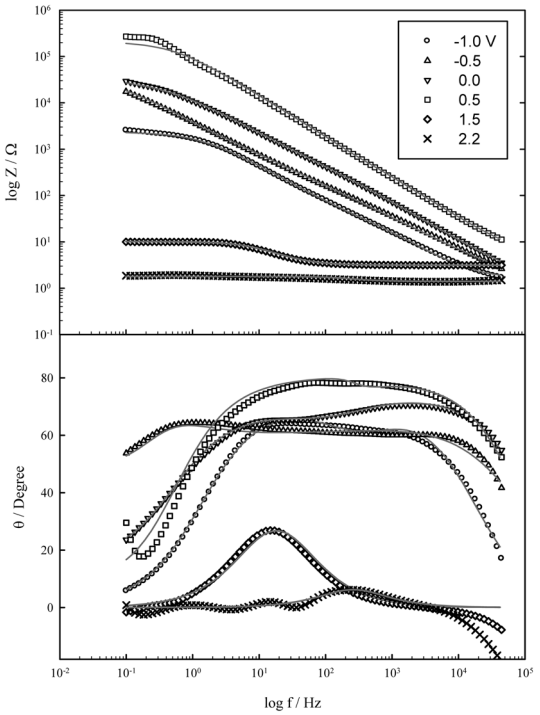

Fig. 4. Bode plots for Pb-1.7%Sb alloy in 5 M H_2SO_4 at different potentials. Plots were recorded after 30 minutes of oxidation. Symbols : Experimental data and Lines : Simulation with the equivalent circuit shown in Fig. 5.

slopes (log Z/log f) of the linear segments are ~ −0.7. For diffusion controlled processes, Bode slope should be −0.5 and for charge transfer controlled processes the slope should be −1.0.[42,41] Thus, a mixed control (diffusional + activational) is assumed at $E_{ox} \leq 0.5$ V. At $E_{ox} \geq 1.5$ V the plots are not linear and shift to much lower impedance values and they signify the formation of the conducting PbO_2. Bode plots in Fig. 4 were satisfactory fitted using the equivalent circuit given in Fig. 5. The elements of the proposed equivalent circuit are the double layer capacitance of electrode/electrolyte interface, C_{dl}, the passive film capacitance, C_f, and its resistance, R_f, the charge transfer resistance, R_{ct}, and the diffusion "Warburg" impedance, Z_W, with the Warburg parameter, W, and the solution resistance, R_{sol}. Elements C_{dl} and C_f were treated as non-ideal capacitors and estimated as constant phase elements (CPEs).[43] CPE is characterized by the capacitance part in Farads and a dimensionless exponent part between 1 and 0. CPE is used instead of the conventional capacitance (with exponent part of 1) to account for the surface heterogeneity and usually revealed better fitting of the experimental data with the appropriate equivalent circuit. The speed and nature of the redox process at the interface between the alloy and the solution are characterized by the speed of the charge transfer in terms of R_{ct} and the speed of the mass transfer of reacting soluble species in solution in terms of Z_w. The surface is assumed to be almost covered by a layer of the corrosion product the electronic properties of which is given in terms of C_f and R_f. Z_w is inversely proportional to the diffusion coefficient of the reacting soluble species and hence, the diffusion properties of the passive layer on alloy surface can be deduced.[42]

Fig. 6 shows the dependence of the fitting elements on E_{ox} in the absence and the presence of H_3PO_4. The large effect of E_{ox} on all elements, except R_{sol} and C_{dl}, indicates the formation of different compounds at the different

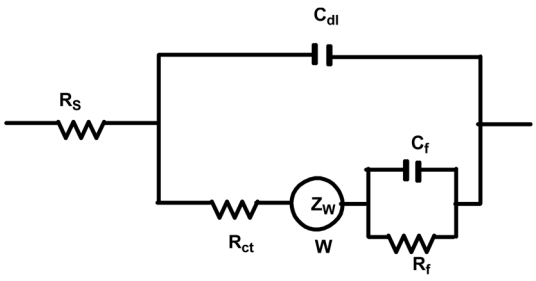

Fig. 5. Equivalent circuit used in the simulation of the impedance data in Fig 4.

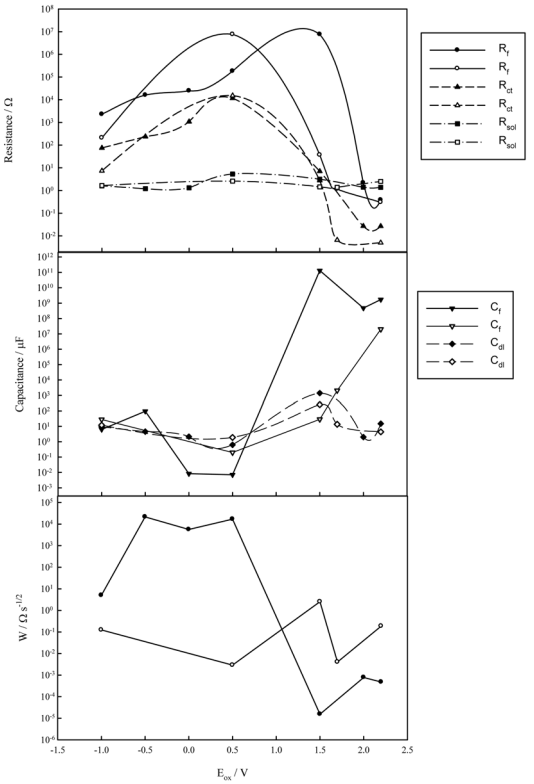

Fig. 6. Fitting elements vs. oxidation potential, E_{ox}, for Pb-1.7%Sb alloy in 5 H_2SO_4 in the absence (Closed symbols) and the presence of 0.4 M H_3PO_4 (Open symbols).

potentials. These surface compounds have significantly different electronic properties, depending on the oxidation potential, and these differences are reflected mainly in C_f, R_f and W.

The effect of addition of H_3PO_4 on R_{ct}, C_{dl} and R_{sol} is less significant compare to its effect on the elements of the passive film properties, R_f, C_f and W. This indicates a significant change in the composition of the passive layer in the presence of H_3PO_4 most probably via thinning of the $PbSO_4$ layer and/or the co-deposition of $PbHPO_4$.

At −1.0 V where a passive $PbSO_4$ layer on the alloy surface is assumed,[39,40] the addition of H_3PO_4 leads to a relative decrease in R_f , a decrease in W and an increase in C_f (cf. curves in the absence and the presence of H_3PO_4 in Fig. 6). These changes indicate a thinner and less protective $PbSO_4$ layer in the presence of H_3PO_4.

At 0.5 V, there is a greater effect of H_3PO_4, where relatively higher R_f and C_f and much lower W values can be seen. It is assumed that the formation of $PbHPO_4$ is the reason behind the significant changes, especially the diffusion characteristics of the passive layer. Previous reports on oxidation of Pb alloys in H_3PO_4 have indicated that the passive layer containing $PbHPO_4$ is porous[20, 21] and this may explain the lower W values in the H_3PO_4-containing solution recorded in the present study. Since the Warburg parameter is inversely proportional to the square root of the diffusion coefficient(s) of the soluble species involved in the redox process,[42] one can deduce that the effective diffusion coefficient(s) of soluble species through the passive layer containing $PbHPO_4$ is (are) higher than those in the H_3PO_4-free solution.

At ≥ 1.5 V, the formation of the conducting PbO_2 prevails and a substantial increase in C_f and a concurrent decrease in R_f can be seen in Fig. 6. The much higher C_f values in H_3PO_4-free in the region of PbO_2 formation at potentials ≥ 1.5 V support the conclusion of the retardation of PbO_2 formation in the presence of H_3PO_4. W values are several orders of magnitude lower, i.e. the diffusion through PbO_2 is much easier than through the passive layer at lower oxidation potentials. This means that the PbO_2 layer is much porous than the insulating $PbSO_4$ at lower oxidation potentials. In the presence of H_3PO_4, however, the diffusion through PbO_2 layer is more difficult. This may be explained in terms of a thinner but more compact PbO_2 layer in the presence of H_3PO_4.

In conclusion, current and impedance fluctuations recorded, during the potentiostatic oxidation Pb-1.7%Sb alloy in 5 M H_2SO_4 at 0.5 V-1.7 V, are attributed to the transformations of the insulating Pb(II) species into the conducting PbO_2. These fluctuations are suppressed in the presence of H_3PO_4 due to the formation of $PbHPO_4$. The insulating properties of $PbSO_4$ layer in the presence of H_3PO_4 are inferior to those in H_2SO_4 alone and the $PbSO_4$ amount is less. Also, the amount of PbO_2 formed in the presence of H_3PO_4 is less than in the H_3PO_4-free solution. The diffusion in the passivity region (−1.0 V to 0.5 V) is more facile in the presence of H_3PO_4 while in the region of PbO_2 formation (≥ 1.5 V) diffusion is more difficult compared to H_3PO_4-free solution.

3.2. Self-discharge in the absence and the presence of H_3PO_4

3.2.1. Long oxidation period

Pb-1.7%Sb alloy was oxidized at 2.3 V for 15 minutes in 5 M H_2SO_4 in the absence and the presence of H_3PO_4, then the polarization circuit was switched off and the open circuit potential, E_{oc}, C and R were followed for a few hours. As can be seen in Fig. 7, E_{oc}, C and R decrease

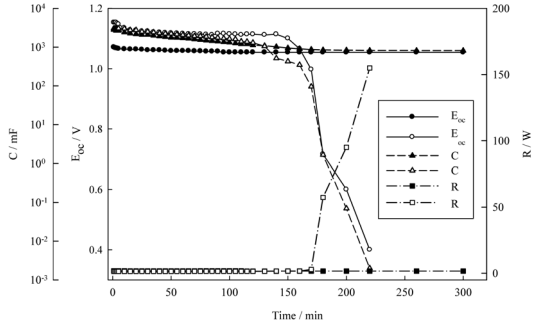

Fig. 7. Variation of open-circuit potential, E_{oc}, capacitance, C, and resistance, R with time in 5 M H_2SO_4 in the absence (Closed symbols) and the presence of 0.4 M H_3PO_4 (Open symbols) during the self-discharge of Pb-1.7%Sb alloy after its oxidation at 2.3 V for 15 minutes.

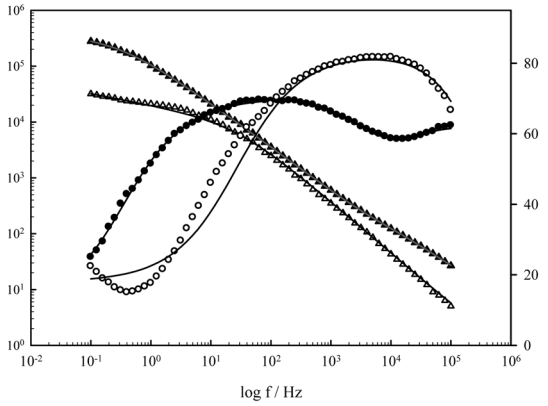

Fig. 8. Bode plots for Pb-1.7%Sb alloy in 5 M H_2SO_4 in the absence (Closed symbols) and the presence of 0.4 M H_3PO_4 (Open symbols). Alloy was pre-oxidized at 2.3 V for 15 minutes. Plots were recorded at the quasi-steady E_{oc} after 24 hours of self-discharge. Circles) Z and triangles) θ. Lines are the simulations according to the equivalent circuit in Fig. 5.

slightly in the H_3PO_4–free solution over the period of five hours, but they start to change sharply after about two hours in the presence of H_3PO_4. The fact that C decreases, R increases and E_{oc} shifts to less positive potentials is a clear indication of the self-discharge of the conducting PbO_2 into the insulating basic $PbSO_4$ and $PbSO_4$. The following processes may occur in the self-discharge process of PbO_2:[44-47]

a) Oxidation of the underlying Pb in the alloy:

$$Pb + PbO_2 + 2H_2SO_4 \rightarrow 2PbSO_4 + 2H_2O \quad (1)$$

b) Oxidation of hydrogen dissolved in solution:

$$PbO_2 + H_2 + H_2SO_4 \rightarrow PbSO_4 + 2H_2O \quad (2)$$

c) Evolution of O_2:

$$PbO_2 + H_2SO_4 \rightarrow PbSO_4 + H_2O + ½\ O_2 \quad (3)$$

Reaction (1) is the main way of the self-discharge and the reason of the gradual degradation of the anode grid in service. The results suggest that the addition of H_3PO_4 accelerates the self-discharge process. The faster self-discharge in H_3PO_4 may be attributed to either of the following two reasons or both: 1- The amount of PbO_2 formed in the presence of H_3PO_4 is already smaller and consequently the time needed for the self-discharge is shorter. 2- H_3PO_4 has negligible effect on the formation of PbO_2 but it influences the chemical composition and properties of the PbO_2 layer. The results in the previous part (3.1) support the two reasons. Further evidences can be obtained from EIS data recorded after the full self-discharge of PbO_2 (after 24 hours) in the absence and the presence of H_3PO_4 (Fig. 8). The estimated R_f, C_f and W without (with) H_3PO_4 from these plots are, respectively: 329.5 kΩ (183.4 kΩ), 98.3 nF (494.5 nF) and 40.4 kΩ s^{-1} (178.7 Ω s^{-1}). Higher R_f and lower C_f in the H_3PO_4-free solution indicate either a thicker passive film or better insulating properties of the passive layer. The large difference in W values cannot be explained by considering the effect of thickness only, and structural changes of the passive layer should be considered.

3.2.2. Short oxidation period

The effect of H_3PO_4 on the initial stage of oxidation was studied by oxidizing Pb-1.7%Sb alloy at 2.0 V for 10, 30 or 60 seconds, then opening the circuit and recording E_{oc}, C and R during the self-discharge process. As can be seen from Fig. 9, the low E_{oc} values in the H_3PO_4-free solution after oxidation for 10 and 30 seconds ($E_{oc} \leq$ 0.08 V and $E_{oc} \leq 0.3$ V, respectively) with their corresponding C and R changes indicate the initial absence of PbO_2 before the self-discharge. At these conditions only $PbSO_4$ is formed on oxidation. After 60 seconds of oxidation, E_{oc} stays high ~1.1 V for 55 minutes before it starts to decreases sharply with a concurrent decrease in C and an increase in R, due to the transformation of the conducting PbO_2 to the insulating mixture of PbO and $PbSO_4$.[47] Addition of H_3PO_4 has two effects: 1- The PbO_2 formation is possible after 30 seconds of oxidation and consequently, H_3PO_4 shortens the time period of $PbSO_4$ formation before the start of the transformation of $PbSO_4$ into PbO_2. 2- The amount of PbO_2 formed at 60 seconds is smaller than that in the H_3PO_4-free solution. The two effects are reflected in a faster decrease in E_{oc} and C and a

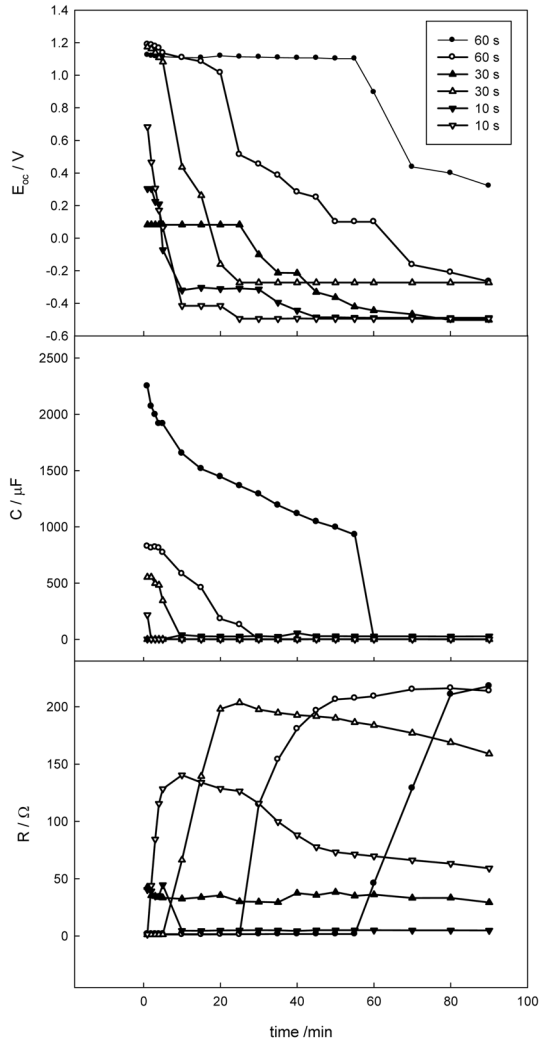

Fig. 9. Variation of open-circuit potential, E_{oc}, capacitance, C, and resistance, R with time in 5 M H_2SO_4 in the absence (Closed symbols) and the presence of 0.4 M H_3PO_4 (Open symbols) during the self-discharge of Pb-1.7%Sb alloy after its oxidation at 2.0 V for different times.

faster increase in R in the presence of H_3PO_4.

Impedance spectra after 6 hours of self-discharge (practically full self-discharge) were recorded at E_{oc} for Pb-1.7%Sb alloy after its oxidation for 10, 30 and 60 seconds in 5 M H_2SO_4 in the absence and the presence of 0.4 M H_3PO_4. As can be seen in Fig. 10, Z values after 10 and 30 seconds of oxidation in the absence of H_3PO_4 are significantly lower than in the other cases. This supports the absence of PbO_2 layer under these oxidation conditions. In general, Z shifts towards higher

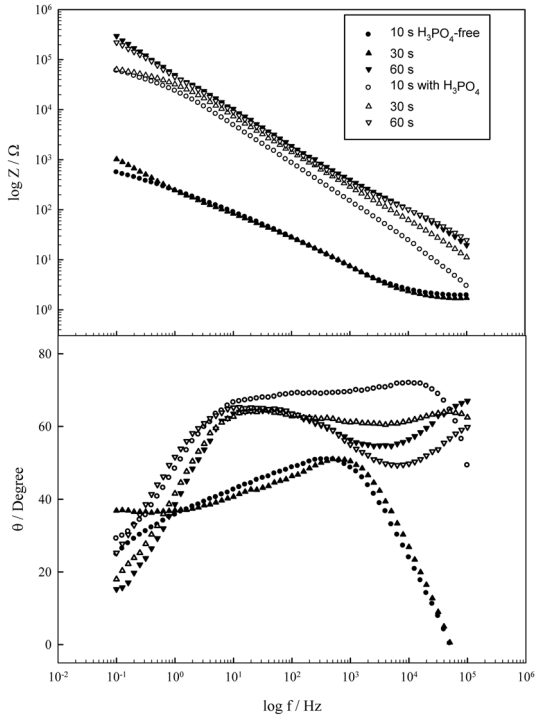

Fig. 10. Bode plots for Pb-1.7%Sb alloy at the quasi-steady E_{oc} in 5 M H_2SO_4 in the absence (Closed symbols) and presence of 0.4 M H_3PO_4 (Open symbols). Alloy was pre-oxidized at 2.0 V for different times and then self-discharged for five hours before recording the Bode plots.

values as t_{ox} increases. The magnitude of Z after 10 seconds of oxidation in the presence of H_3PO_4 indicates that a small amount PbO_2 is formed (could not be detected in the self-discharge curves of Fig. 9).

Fig. 11 shows the dependence of the fitting elements of Bode plots of Fig. 10 on t_{ox}. Generally, the difference between the elements in the absence and the presence of H_3PO_4 at $t_{ox} = 60$ seconds is small, where the formation of PbO_2 during oxidation occurs in both solutions. R_f increases with t_{ox} in both solutions, but it is considerably higher in the presence of H_3PO_4. C_f behavior is consistent with that of R_f and they reflect the thickness of the insulating layer formed after the full discharge. Both R_f and C_f support the absence of PbO_2 at $t_{ox} < 60$ seconds in the H_3PO_4-free solution. The properties of the passive layer formed after full self-discharge are reflected also in R_{ct} behavior. R_{ct} increases with t_{ox} in the H_3PO_4-free solution but it deceases in the presence of H_3PO_4. At $t_{ox} < 60$ seconds R_{ct} is higher in the presence of H_3PO_4 but at $t_{ox} = 60$ seconds R_{ct} is lower. R_{ct} behavior can be explained

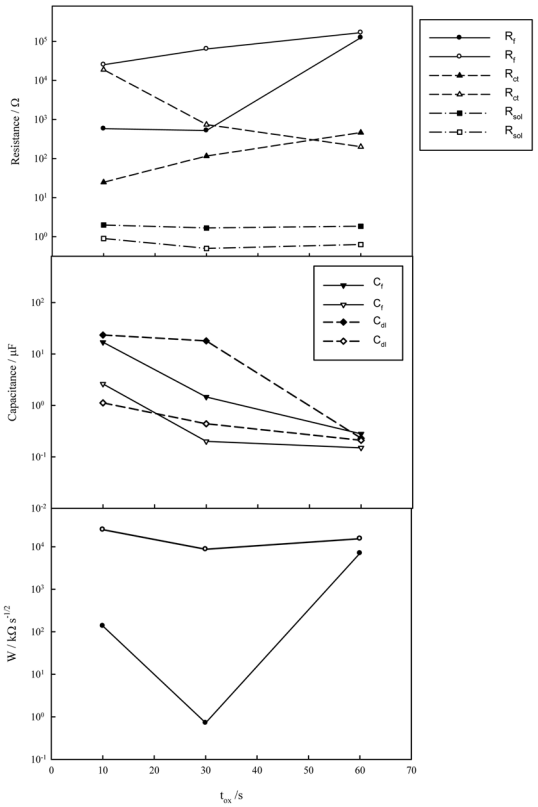

Fig. 11. Fitting elements vs. oxidation time, t_{ox}, for Pb-1.7%Sb alloy in 5 M H_2SO_4 in the absence (Closed symbols) and the presence of 0.4 M H_3PO_4 (Open symbols). Details are in Fig. 10.

as follows: In the absence of H_3PO_4, as t_{ox} increases a thicker barrier film is formed and consequently R_{ct} increases. In the presence of H_3PO_4, as t_{ox} increases a thicker but a less protective barrier film (contains $PbHPO_4$) is formed and alternatively R_{ct} decreases. Deterioration of the protection properties of the passive film in the presence of H_3PO_4 seems to be limited because W in the presence of H_3PO_4 is still higher (i.e. more difficult diffusion) than in the H_3PO_4-free solution, though the difference at t_{ox} = 60 seconds is not very high.

In conclusion, the self-discharge experiments indicate that the efficiency of PbO_2 formation is higher in the H_3PO_4-free solutions, i.e. H_3PO_4 retards the formation of PbO_2. However, short oxidation times (less than a minute at 2.0 V) reveal that H_3PO_4 shortens the period of $PbSO_4$ layer formation and enhance the start of PbO_2 transformation. When oxidation time is sufficiently larger than the time needed for formation of $PbSO_4$ layer (~a minute at 2.0 V), H_3PO_4 shows its retardation effect of formation of PbO_2.

References

1. S. Tudor, A. Weisstuch, and S. H. Davang, *Electrochem. Technol.*, **5**, 21 (1967).
2. J. Burbank, *J. Electrochem. Soc.*, **111**, 1112 (1964).
3. B. K. Mahato, *J. Electrochem. Soc.*, **126**, 369 (1979).
4. E. Voss, *J. Power Sources*, **24**, 171 (1988).
5. H. A. Laitinen and N. Walkins, Anal. Chem., **47**, 1353 (1975).
6. K. R. Bullock, *J. Electrochem. Soc.*, **126**, 1848 (1979).
7. S. Tudor, A. Weisstuch and S.H. Davang, *Electrochem. Technol.*, **4**, 406 (1966).
8. S. Tudor, A. Weisstuch, and S. H. Davang, *Electrochem. Technol.*, **3**, 90 (1965).
9. K. R. Bullock and D. H. McClelland, *J. Electrochem. Soc.*, **124**, 1478 (1977).
10. K. R. Bullock, *J. Electrochem. Soc.*, **126**, 360 (1979).
11. S. Stemberg, A. Mateescu, V. Branzoi, and L. Apateanu, *Electrochim. Acta,* **32**, 349 (1987).
12. W. Visscher, *J. Power Sources*, **1**, 257 (1976/77).
13. H. Doring, K. Wiesener, J. Garche, and P. I. Fischer, *J. Power Sources*, **38**, 261 (1992).
14. S. Sternberg, V. Branzoi, and L. Apateanu, *J. Power Sources*, **30**, 177 (1990).
15. J. Garche, H. Doring, and K. Wiesener, *J. Power Sources*, **33**, 213 (1991).
16. S. Venugopalan, *J. Power Sources*, **46**, 1 (1993).
17. S. Venugopalan, *J. Power Sources*, **48**, 371 (1994).
18. E. Meissner, *J. Power Sources*, 67, **135** (1997).
19. A. Bhattacharya and I. N. Basumallick, *J. Power Sources*, **382** (2003).
20. I. Paleskaa, R. Pruszkowska-Drachala, J. Kotowskia, A. Dziudzia, J. D. Milewskic, M. Kopczykc, and A. Czerwinskia, *J. Power Sources*, **113**, 308 (2003).
21. S. Li, H. Y. Chen, M. C. Tang, W. W. Wei, Z. W. Xia, Y. M. Wu, W. S. Li and X. Jiang, *J. Power Sources*, **158**, 914 (2006).
22. K. Saminathan, N. Jayaprakash, B. Rajeswari and T. Vasudevan, *J. Power Sources*, **160**, 1410 (2006).
23. I. M. Ismail and A. H. El Abd, *Chem. Age India*, **34**, 393 (1983).
24. Yu. A. Zinchenko, O. L. Aleksandrova, M. R. Biegul, A. 1. Petrukhova and V. D. Bar'Sukov, *Tovarnye Znaki*, **48**, 1194 (1971).
25. W. A. Badawy and S. S. El-Egamy, *J. Power Sources*, **55**, 11 (1995).
26. B.K. Mahato and W.H. Tiedemann, *J. Electrochem. Soc.*, 130, 2139 (1983).
27. L. T. Lam, J. D. Douglas, R. Pilling and D. A. J. Rand, *J. Power Sources*, **48**, 219 (1994).
28. H. Sanchez, Y. Meas, I. Gonzalez and M. A. Quiroz, *J. Power Sources*, **32**, 43 (1990).
29. M. Maja and N. Penazzi, *J. Power Sources*, **22**, 1 (1988).

30. K. Mc Gregor, *J. Power Sources*, **59**, 31 (1996).
31. D. Pavlov, *J. Power Sources*, **33**, 221 (1991).
32. D. Pavlov, A. Dakhouche and T. Rogachev, *J. Power Sources*, **42**, 71 (1993).
33. D. Pavlov, *J. Power Sources*, **46**, 171 (1993).
34. T. Rogachev and D. Pavlov, *J. Power Sources*, **64**, 51 (1997).
35. N. Chahmanaa, M. Matrakovab, L. Zerroual and D. Pavlov, *J. Power Sources*, **191**, 51 (2009).
36. N. Chahmana, L. Zerroual and M. Matrakova, *J. Power Sources*, **191**, 144 (2009).
37. M. Ghaemi, E. Ghafouri and J. Neshati, *J. Power Sources*, **157**, 550 (2006).
38. A. G. Gad-Allah, H. A. Abd El-Rahman, S. A. Salih and M. Abd El-Galil, *Thin Solid Films*, **213**, 244 (1992).
39. A. G. Gad-Allah, H. A. Abd El-Rahman, S. A. Salih and M. Abd El-Galil, *J. Appl. Electrochem.*, **22**, 571 (1997).
40. R. Greef, R. Peat, L. M. Peter, D. Pletcher, J. Robinson, In: *Instrumental Methods in Electrochemistry*, pp. 298-312, Ellis Horwood, London (1990).
41. A. J. Bard L. R. Faulkner, *Electrochemical Methods Fundamentals and Applications*, 2nd Ed., Ch.10, Wiley, New York (2001).
42. M. Metikos-Hukovic, R. Babic and S. Brinic, *J. Power Sources*, **157**, 563 (2006).
43. V. Lliev, D. Pavlov, *J. Electrochem. Soc.*, **129**, 1393 (1982).
44. J. S. Symanski, B. K. Mahato and K. R. Bullock, *J. Electrochem. Soc.*, **135**, 548 (1988).
45. D. Pavlov, I. Balkamov and P. Rachev, *J. Electrochem. Soc.*, **134**, 2390 (1987).
46. A. G. Gad-Allah, H. A. Abd El-Rahman, M. Abd El-Galil, *J. Appl. Electrochem.*, **25**, 682 (1995).